



Undergraduate Honors Theses

---

2020-03-20

## Increasing Isolation Between Closely Spaced X-Band Planar Transmit/Receive Antennas

Jacob Bartschi

Follow this and additional works at: [https://scholarsarchive.byu.edu/studentpub\\_uht](https://scholarsarchive.byu.edu/studentpub_uht)



Part of the [Electrical and Computer Engineering Commons](#)

---

### BYU ScholarsArchive Citation

Bartschi, Jacob, "Increasing Isolation Between Closely Spaced X-Band Planar Transmit/Receive Antennas" (2020). *Undergraduate Honors Theses*. 110.  
[https://scholarsarchive.byu.edu/studentpub\\_uht/110](https://scholarsarchive.byu.edu/studentpub_uht/110)

This Honors Thesis is brought to you for free and open access by BYU ScholarsArchive. It has been accepted for inclusion in Undergraduate Honors Theses by an authorized administrator of BYU ScholarsArchive. For more information, please contact [ellen\\_amatangelo@byu.edu](mailto:ellen_amatangelo@byu.edu).

Honors Thesis

INCREASING ISOLATION BETWEEN CLOSELY SPACED  
X-BAND PLANAR TRANSMIT/RECEIVE ANTENNAS

By

Jacob Bartschi

Submitted to Brigham Young University in partial fulfillment of graduation requirements for  
University Honors

Electrical Engineering Department

Brigham Young University

April 2020

Advisor: Karl Warnick

Honors Coordinator: Karl Warnick



# ABSTRACT

## INCREASING ISOLATION BETWEEN CLOSELY SPACED X-BAND PLANAR TRANSMIT/RECEIVE ANTENNAS

Jacob Bartschi

Electrical Engineering Department

Bachelor of Science

Coupling between Tx/Rx antennas is a common and much-researched problem that is especially difficult when the antennas both placed close together and on the same plane. New systems with smaller footprints require this kind of placement while still maintaining the same levels of isolation as before. Traditional solutions for coupling involve large and heavy machined parts that are unsuited to compact systems. Many techniques have been proposed over the decades, but few have been applied to X-band antennas in closely spaced configurations. This thesis investigates those techniques, applies them to closely spaced X-band antennas, and compares them to conventional methods of increasing isolation. Recommendations are made on what techniques are observed to work best for this scenario.



## ACKNOWLEDGEMENTS

I would like to acknowledge the BYU Smart Antenna Systems research group for introducing me to the wonderful field of RF and electromagnetics and teaching me how to be a researcher. I would especially like to thank Dr. Karl Warnick for his guidance and support throughout my education and in this thesis. Finally, I thank my wife for her patience and encouragement to follow through with difficult things.



# TABLE OF CONTENTS

TITLE .....	i
ABSTRACT.....	iii
ACKNOWLEDGEMENTS.....	v
TABLE OF CONTENTS.....	vii
LIST OF TABLES AND FIGURES.....	ix
1 Introduction.....	1
1.1 Literature Review.....	2
2 Common Isolation Solutions.....	5
2.1 Increasing Distance Between Antennas .....	5
2.2 Via Shielding .....	7
3 Low Insertion Loss Filters .....	11
3.1 Defected Ground Plane Filters.....	11
3.2 Defected Microstrip Filters .....	13
4 Isolation by Physical Barriers .....	15
4.1 Variation in Material.....	15
4.2 Variation in Barrier Shape .....	21
4.3 Variation in Barrier Placement .....	25
5 Isolation by Electromagnetic Band Gap Structures .....	27
5.1 Mushroom-Like EBG .....	27
5.2 UC-EBG.....	30
5.3 AI-EBG .....	32
6 Comparison of the Investigated Techniques.....	35
7 Conclusions.....	37
7.1 Further Research .....	37



References.....	38
-----------------	----

## LIST OF TABLES AND FIGURES

Figure 2-1: Simulation model of control. Two 10GHz patch antennas on a shared substrate separated by one wavelength.....	5
Figure 2-2: Simulation model of control antennas on the same substrate separated by 10 wavelengths.....	6
Figure 2-3: Simulation model of control antennas on separate substrate separated by 10 wavelengths of air. ....	6
Figure 2-4: Mean in-band coupling between control antennas at varying separation. Coupling decreases dramatically as separation increases. ....	7
Figure 2-5: Simulation model of control antennas spaced 1 wavelength apart separated by a via wall. ....	8
Figure 2-6: Mean in-band coupling between control antennas separated by rows of vias. Inserting via walls does not demonstrate a decrease in coupling. ....	9
Figure 3-1: Design of DGS U-slots. This structure would be etched from the ground plane underneath the microstrip trace. ....	12
Figure 3-2: Prototyped double slot DGS filter.....	12
Figure 3-3: Prototyped DMS filter. Note that the pictured filter is intended to be a microstrip line rather than the coplanar waveguide seen. The top ground plane was removed later to test the filter as intended. ....	13
Figure 4-1: Comparison of coupling by barrier materials. In this test, the FR4 showed the best increase in isolation. ....	20
Figure 4-2: Increase in coupling when using an inductive coil. ....	21
Figure 4-3: Simulations models of metal grating barrier with variable number of sheets. More of the radiated waves are blocked as the number of sheets increases.....	26
Figure 5-1: Performance of EBG barrier from [10], demonstrating an average decrease in coupling of about 7dB in the band of interest .....	28
Figure 5-2: Mushroom-like EBG unit cell reflection phase. At a reflection phase of 0, the unit cell acts as a perfect magnetic conductor, indicating where the center frequency of the band gap will be when the unit cell is integrated into a periodic structure. ....	28
Figure 5-3: Mushroom-like EBG barrier simulation model. Two control antennas are separated by 10 wavelengths and a 4x4 periodic EBG structure.....	29

Figure 5-4: Coupling between antennas with mushroom-like EBG barrier. Isolation is increased by an average of 4.4dB over the 10-10.5 GHz band. ....	29
Figure 5-5: UC-EBG unit cell reflection phase. At a reflection phase of 0, the unit cell acts as a perfect magnetic conductor, indicating where the center frequency of the band gap will be when the unit cell is integrated into a periodic structure.....	30
Figure 5-6: UC-EBG simulation model. Two control antennas are separated by 10 wavelengths and a 4x4 periodic EBG structure. ....	31
Figure 5-7: Coupling between antennas with UC-EBG barrier. Isolation is increased by an average of 2dB over the 10-10.5 GHz band. ....	31
Figure 5-8: AI-EBG unit cell reflection phase. At a reflection phase of 0, the unit cell acts as a perfect magnetic conductor, indicating where the center frequency of the band gap will be when the unit cell is integrated into a periodic structure.....	32
Figure 5-9: AI-EBG simulation model. Two control antennas are separated by 10 wavelengths and a 4x4 periodic EBG structure. ....	33
Figure 5-10: Coupling between antennas with AI-EBG Barrier. Isolation is increased by an average of 2.9dB over the 10-10.5 GHz band. ....	33
Table 1: Effectiveness of decoupling by vias. ....	9
Table 2: Simulation of increase in isolation by material.....	16
Table 3: Physical testing of barrier materials.....	18
Table 4: Simulation of metal barrier isolation by shape. ....	22
Table 5: Simulation of metal barrier isolation by configuration.....	24
Table 6: Comparison of isolation techniques.....	35

# 1 Introduction

As communications technology shrinks further and further, one of the hard limits on receive sensitivity is saturation from the transmit antenna on the same device. Saturation happens when an unwanted signal drowns out a desired signal, like when one person shouting in a room can make other conversations harder to hear. When antennas are placed close together, they can couple and cause saturation. Electromagnetic coupling occurs when an electromagnetic field created by charges traveling through one medium creates electrical charge onto a separate medium. In circuits, this often takes the form of a high frequency signal in one wire or trace creating noise in an unrelated wire or trace. This kind of unwanted coupling degrades the performance of the system, corrupting information or preventing desired signals altogether, and coupling between antennas is a major contributor to saturation. Saturation due to antenna coupling decreases the effective range of receive devices as well as restricts the potential output power of transmit systems. In practice, this can mean that a radar will not be able to detect as far, or a satellite might not communicate with the ground

Compact planar antennas are especially susceptible to coupling. Not only do planar antennas often have significant sidelobes that cause signal to bleed over undesirably into another antenna, but often these planar antennas are built on the same printed circuit board, increasing the ease in which that coupling occurs. In a communication device or a radar, the transmit signal can overwhelm the return signal that the receive antenna is looking for. Received signals are typically orders of magnitude smaller than a transmit signal, which leads to the effect called saturation, where the receive system cannot separate weak return signals from the transmit signal.

New research in simultaneous receive and transmit (STAR) antennas is not immune to coupling, either. In STAR antennas, both receive and transmit signals are handled in on the same frequency at the same time on the same antenna. While this technology can greatly increase data rates and reduce system size, coupling between the transmit and receive lines can ruin the signal. In this case, the antenna couples with itself rather than a separate antenna.

Much research has been done on increasing electromagnetic isolation between components, especially antennas. Traditional solutions for coupling involve large and heavy machined parts that are unsuited to compact systems. On the other hand, many modern solutions involve complicated and precise phase-cancelling methods. These techniques involve redirecting a portion of the transmit signal and mixing into the receive signal and are extraordinarily effective when implemented digitally, but they are power hungry and computationally taxing. These constraints

may cause those software techniques to be unattractive for small platforms such as UAS or CubeSats.

When power and computational constraints prevent software solutions, engineers must turn back to hardware design to solve coupling problems. Research in hardware solutions for electromagnetic coupling is very mature, but they have seldom been applied to X-band systems. The X-band, centered around 10 GHz and typically defined as 8-12 GHz, is mostly used by radar and satellite communications. With technology trends of shrinking X-band system sizes, such as the advancement of CubeSat technology for the case of satellites, saturation and coupling continues to be an obstacle to system design at this band. This work will review several existing hardware solutions and apply them to closely spaced planar X-band antennas. In addition, a new solution will be proposed and tested in the form of a metal grating barrier. Each technique will be compared and evaluated for their performance and convenience in implementation.

This thesis will provide a reference for uncommon solutions to coupling in X-band systems and provide design examples of the solutions. It demonstrates the effectiveness of novel methods in solving this problem for planar X-band systems and gives recommendations qualified by the constraints of a given system, comparing them to conventional decoupling methods.

## 1.1 Literature Review

There has already been much work done on the issue of antenna coupling. [1] presented an analysis of the common solution of a physical barrier. [2] used an early decoupling circuit placed in between the feeds of two folded unipole antennas. The circuit was composed of lumped elements and varying lengths of transmission line to cancel the offending signal by combining it with an out-of-phase version of itself. This concept is commonly used in electronics today and is still used for modern antenna systems such as is investigated in [3].

[4] approaches a similar problem of decoupling flush slot antennas that shared a common ground. The paper presented a solution of introducing a lossy dielectric slab between the antennas [5] introduced the use of parasitic elements between antennas to leech off the unwanted signal. The research done in these early works later influenced the development of electromagnetic band gap (EBG) structures [6], which can be seen as a kind of lossy material as discussed in [4] realized with parasitic elements like those used in [5]. The EBG structures, more directly based on photonic band gap structures, are periodic designs that exhibit rejection of a narrow band of frequencies. Early versions were volumetric, requiring vias when implemented in PCB technology. Later

developments introduced planar designs that did not require vias, though they sometimes used multiple parallel planes [7-11]. The principles of these structures were also used to develop low insertion loss filters in the form of defected ground structure (DGS) and defected microstrip (DMS) filters [12-13].

These works typically address communication systems in sub-8 GHz bands and do not extend their solutions to the growing group of X-band systems.



## 2 Common Isolation Solutions

Coupling is not a new problem in the realm of antennas. Common methods of decoupling planar antennas are to either increase the distance between the antennas or to shield using vias. In the following simulations, the simulated coupling between two patches separated by a distance of one wavelength on the same substrate is used as the control measurement.

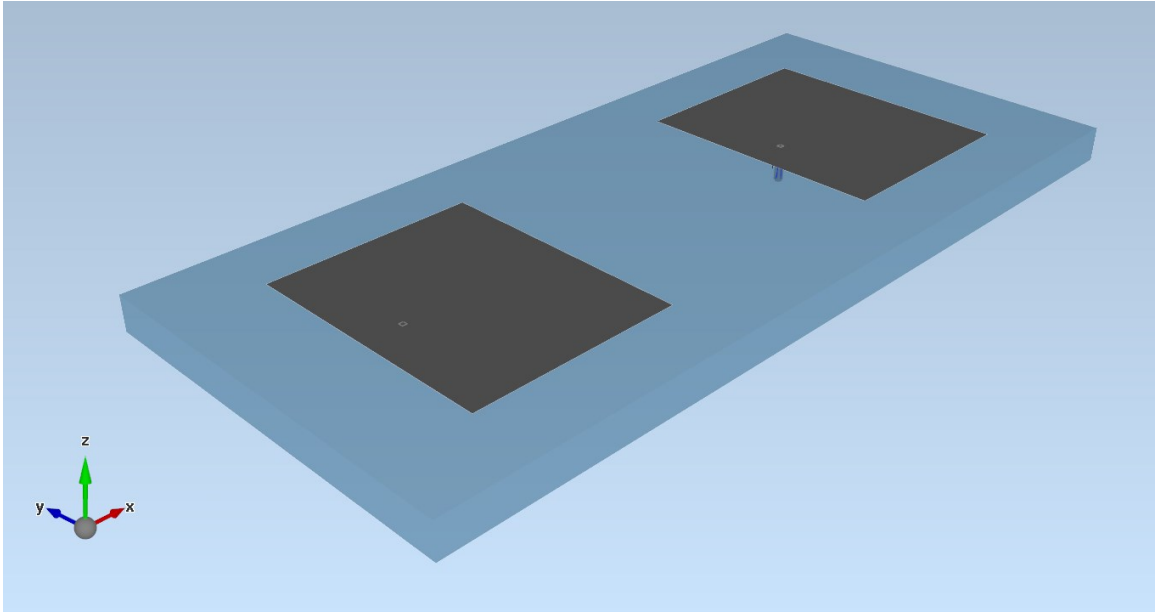


*Figure 2-1: Simulation model of control. Two 10GHz patch antennas on a shared substrate separated by one wavelength.*

### 2.1 Increasing Distance Between Antennas

As an electromagnetic wave travels away from a transmitting source, it decreases in power by the inverse square law. Hence a point 10 meters away from a source will receive 100 times less power than a point 1 meter away. Therefore, coupling between antennas can be significantly decreased simply by increasing the space between them.



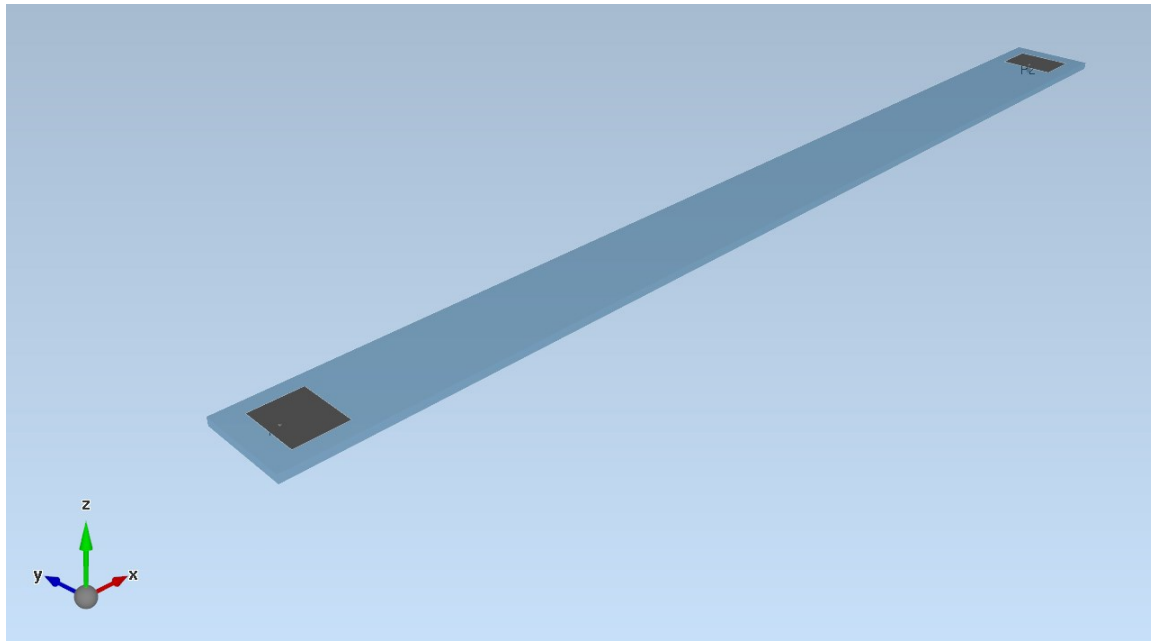


*Figure 2-2: Simulation model of control antennas on the same substrate separated by 10 wavelengths.*

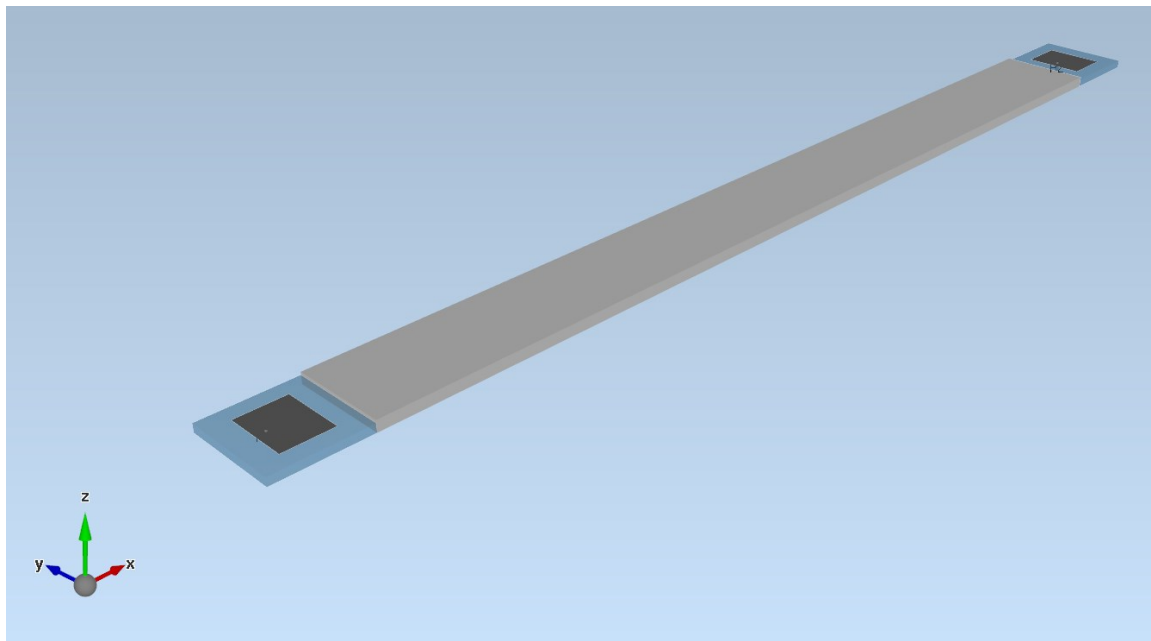


*Figure 2-3: Simulation model of control antennas on separate substrate separated by 10 wavelengths of air.*

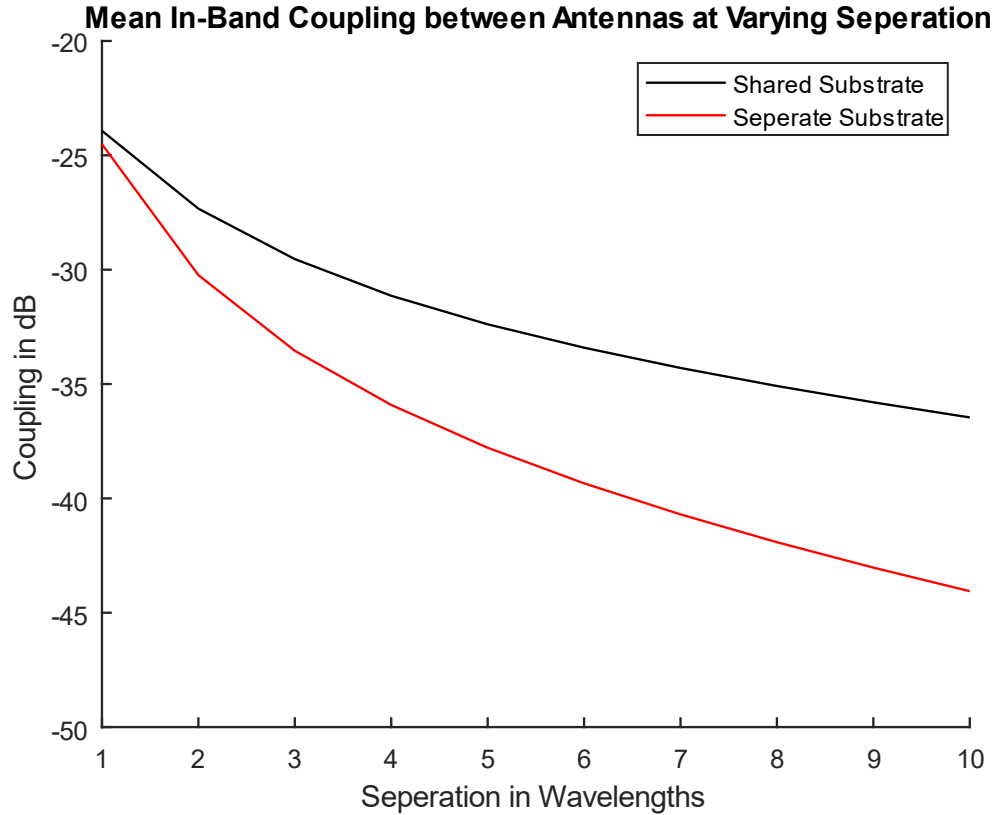


*Figure 2-4: Mean in-band coupling between control antennas at varying separation. Coupling decreases dramatically as separation increases.*

In this simulation, the antennas are most isolated from each other at the max separation simulated, ten wavelengths apart with an increase of isolation of 10dB from one wavelength apart in the case of the shared substrate, and 20dB in the case of the seperate substrate. It can be seen how the isolation would only increase as the antennas are moved even further apart, but real-world applications would naturally limit the use of this technique.

## 2.2 Via Shielding

Planar antennas are often built using printed circuit board (PCB) technologies. Via stitching can be used to shield RF traces and components from unwanted signals propagating through the board. When multiple antennas are built on the same board, via stitching can typically be used to reduce the coupling between the two antennas.

However, when this technique was simulated with closely spaced X-band antennas, the vias increased the coupling. This is thought to be due to them acting as small antennas and reradiating the surface waves from the Tx antennas through the substrate. As such, this technique, while

effectively used to increase isolation between transmission lines, may not always be helpful between planar antennas.

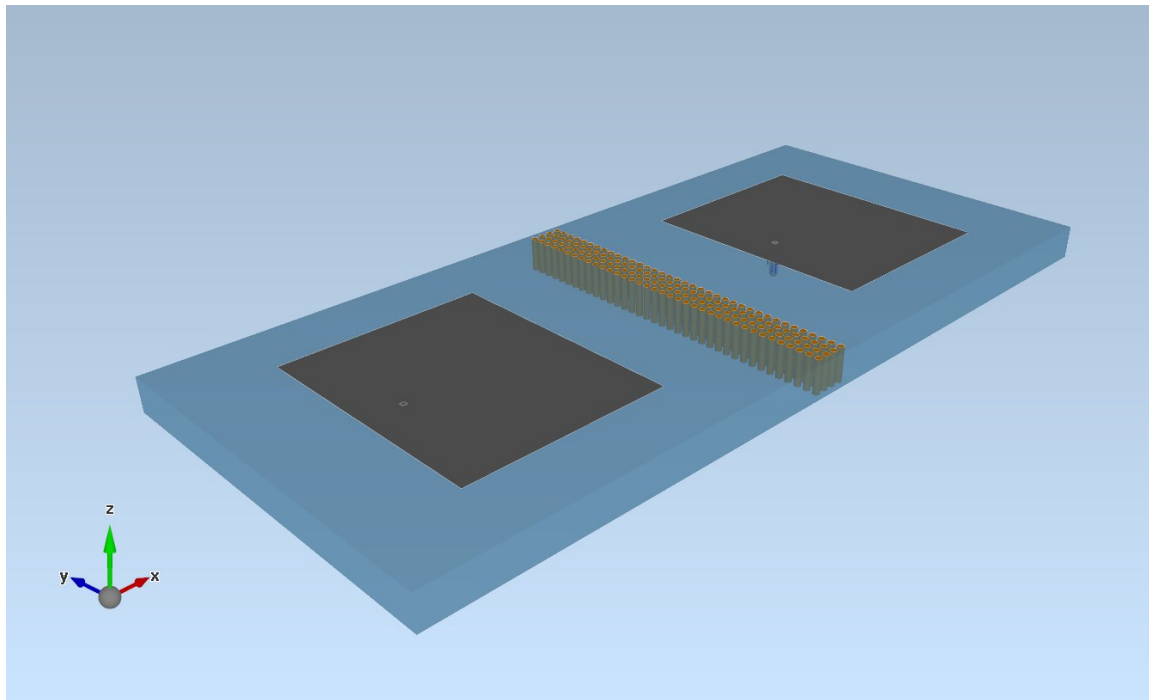


*Figure 2-5: Simulation model of control antennas spaced 1 wavelength apart separated by a via wall.*

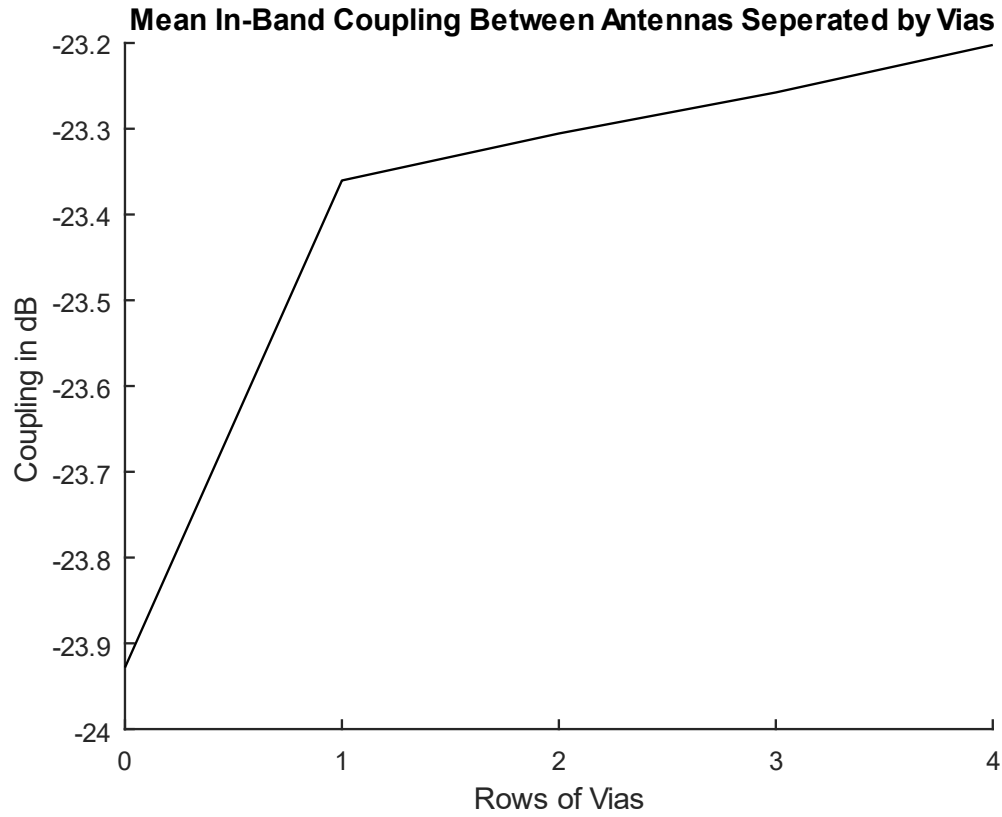


Figure 2-6: Mean in-band coupling between control antennas separated by rows of vias.  
Inserting via walls does not demonstrate a decrease in coupling.

Table 1: Effectiveness of decoupling by vias.

<i>Rows of Vias</i>	<i>Coupling (dB)</i>	<i>Improvement from Control (dB)</i>
<i>Control (No Vias)</i>	-23.93	0
<i>1</i>	-23.36	-0.57
<i>2</i>	-23.31	-0.62
<i>3</i>	-23.26	-0.67
<i>4</i>	-23.20	-0.73



## 3 Low Insertion Loss Filters

When the source of saturation is known, measures can be taken to specifically cancel out that source. In the case of two antennas that are near each other but are listening for different frequencies, special low insertion loss filters can be used to target the unwanted frequencies for the transmit antenna.

For example, a communications satellite will have many antennas communicating on many different frequencies. One antenna might be transmitting in the Ku-Band while another antenna close by might be listening for signals in the X-Band. In this case, the second antenna can be designed to reject those transmitted Ku-band signals. In addition to designing the antenna reject those signals, filters can be used to reject the signals as well. Defected ground plane and defected microstrip filters are especially useful for these applications. They are simple to design and insert into an RF receive chain, and their low insertion loss make them ideal as a first filter in the chain.

### 3.1 Defected Ground Plane Filters

Defected ground plane filters are filters constructed by removing (defecting) the ground plane underneath a microstrip transmission line or antenna in particular patterns [13]. Because they produce a typically narrow rejection band at certain frequencies, they can be considered electromagnetic bandgap (EBG) structures [12], but they will not be referred to as such in this work, as EBG structures will be discussed later on and used in a different way. These structures are highly versatile and can be shaped and cascaded to create nearly any kind of filter [13-16].

Generally, a defected ground plane structure is modeled as a parallel LRC or LC circuit, with the capacitance coming from the gap between the ground plane and microstrip line or antenna, the inductance from the shape of the defect, and the resistance from the loss in the materials [14]. A signal within the rejection band is coupled out of the above structure and into the ground plane.

When trying to increase isolation between antennas, these filters can be used as the 1<sup>st</sup> stage in the RF receive chain [15]. They have extremely low insertion loss (less than 1dB).

#### 3.1.1 *Design of a Defected Ground Plane Filter*

Using commercially available full-wave electromagnetic simulation packages and printed circuit board milling machines, DGS filters can be rapidly designed and prototyped. The following filter for use in a high isolation system was designed by Jakob Kunzler at Brigham Young University [15]. The filter was designed to accept signals in a Rx band of 8.25 – 8.75 GHz and reject signals in a Tx band of 10.25-10.75 GHz.

To begin, a  $50\Omega$  microstrip transmission line with a center frequency of 8.5 GHz was designed on 20mil RO4350 substrate ( $\epsilon_r = 3.66$ ). Then, a U-shaped slot was placed in the ground plane and parameterized by length, width, and thickness. These parameters were adjusted and optimized until a desired performance was achieved in simulation. The final design included a second U-shaped slot nested inside the first. The smaller size created a second reject-band at a frequency slightly higher than the first, effectively widening the reject-band. The filter was prototyped using a PCB mill and tested, and the final design exhibited 25.8dB of rejection in the targeted Tx band.

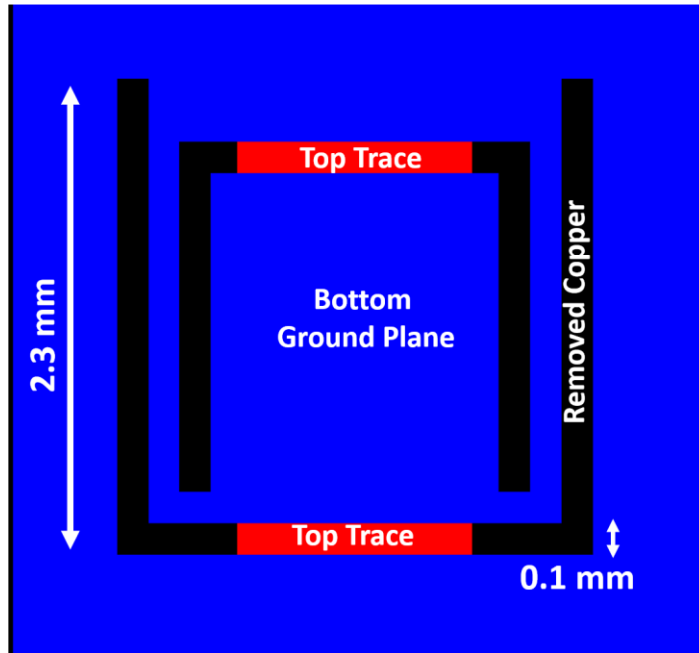


*Figure 3-1: Design of DGS U-slots. This structure would be etched from the ground plane underneath the microstrip trace.*

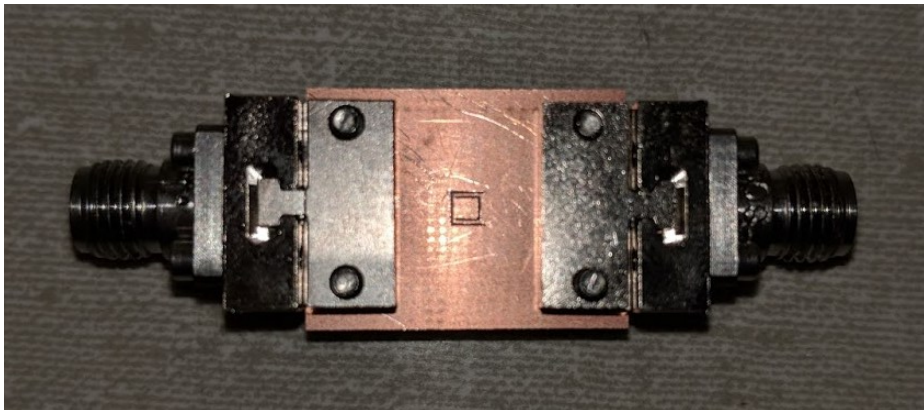


*Figure 3-2: Prototyped double slot DGS filter.*

## 3.2 Defected Microstrip Filters

Defected microstrip filters operate on similar principles to the DGS structures discussed before and have similar performance, producing a notch band-reject filter response [17]. Instead of the defect being etched onto the ground plane of the transmission line, it is etched onto the microstrip line itself.

DMS structure shape is more restricted than DGS shapes, as the structure must fit within the width of the microstrip line. This also means that the structure will radiate out of the top of the microstrip line, rather than out the ground plane as a DGS filter would, which may be more desirable in some applications.

### 3.2.1 Design of a Defected Microstrip Filter

Just as with DGS filters, DMS filters can be quickly designed and fabricated using the same methods. As before, a microstrip line was designed on 20mil RO4350 substrate and a U-shaped slot was placed on the design, this time on the microstrip itself rather than the ground plane. The single U-cut design was prototyped on a PCB mill and produced about 10dB of rejection in the targeted band. By cascading the structure in simulation, the rejection could be increased to match the performance of the DGS filter.

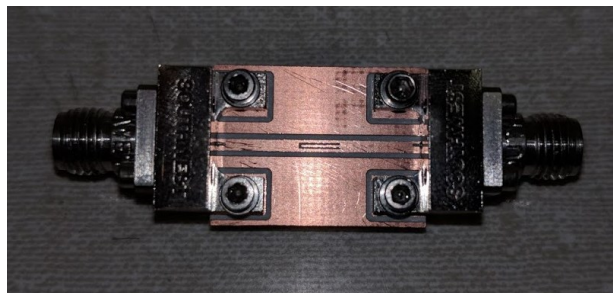


*Figure 3-3: Prototyped DMS filter. Note that the pictured filter is intended to be a microstrip line rather than the coplanar waveguide seen. The top ground plane was removed later to test the filter as intended.*

This design demonstrates the convenience of implementing a band-stop filter on an existing transmission line, provided that the length of line is long enough to fit the defect. It has the advantage over DGS filters in that the ground plane is not interfered with, but it has the disadvantage of requiring a longer area to achieve the same performance.





## 4 Isolation by Physical Barriers

It is commonly known that electromagnetic waves are obstructed by physical media. Thus, isolation can be increased between two antenna simply by placing objects in the path between them. This kind of physical RF barrier was investigated in [1], where a basic barrier of metal plates was analyzed using diffraction theory, then constructed and tested. Modern simulation packages allow for greater analysis of a larger number of barrier materials, shapes, and configurations. The effectiveness of various materials and shapes is discussed below.

### 4.1 Variation in Material

Four materials were considered as barriers:

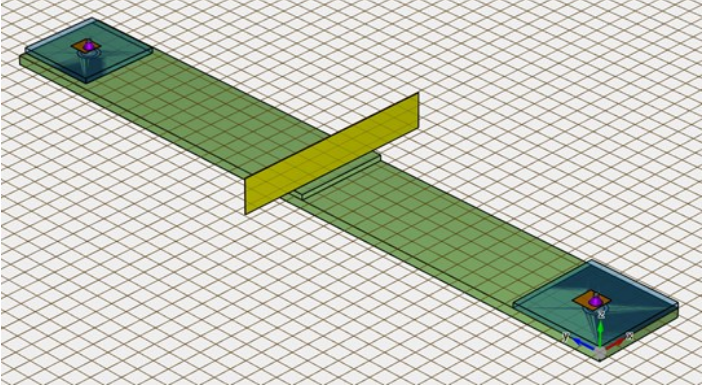
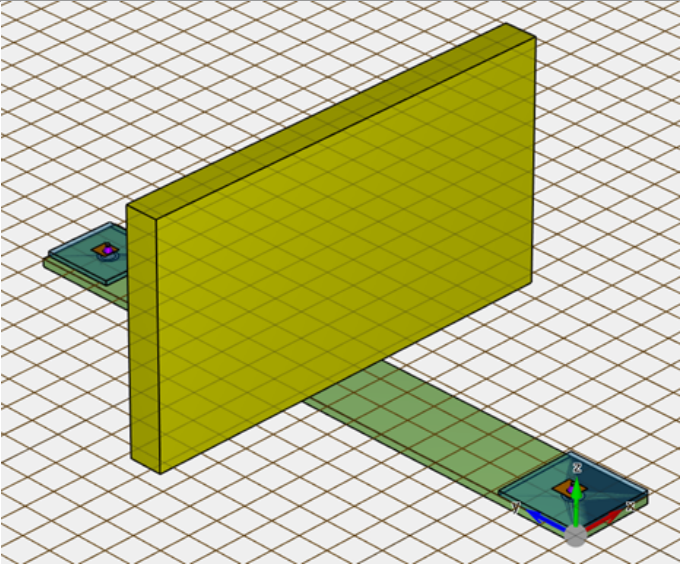
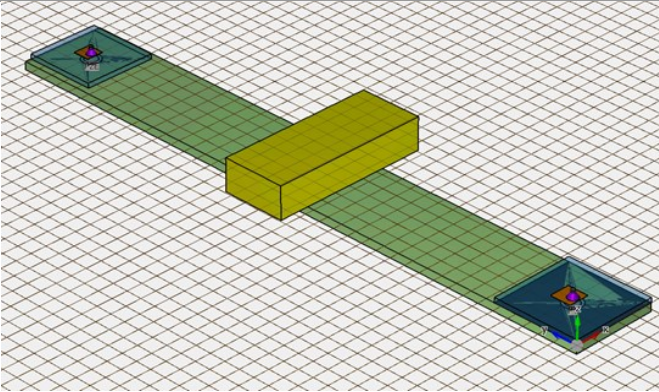
- Conductors (thin sheets of conductive metal)
- RF absorber foam
- FR4 substrate (two copper sheets with FR4 substrate in-between)
- Ferrite

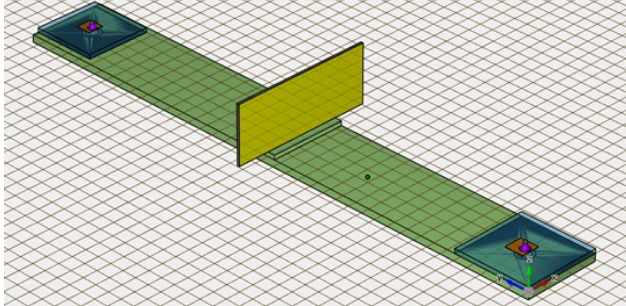
#### 4.1.1 *Simulation of Materials*

These materials were simulated as barriers between two antennas, one tuned to a center frequency of 8.5 GHz, the other tuned to a center frequency of 10.5 GHz, spaced 15cm apart.

In simulation, a simple conductive barrier provided the best increase in isolation and FR4 provided the worst increase out of the materials considered.

Table 2: Simulation of increase in isolation by material.

Material	Increase in Isolation from Control (dB)	Picture
Foil	5.72	
Foam	5.67	
Ferrite (20mm tall x 10mm thick)	2.94	

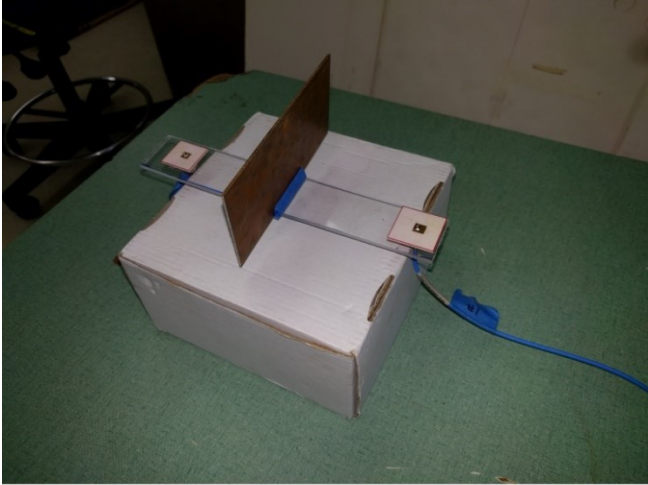
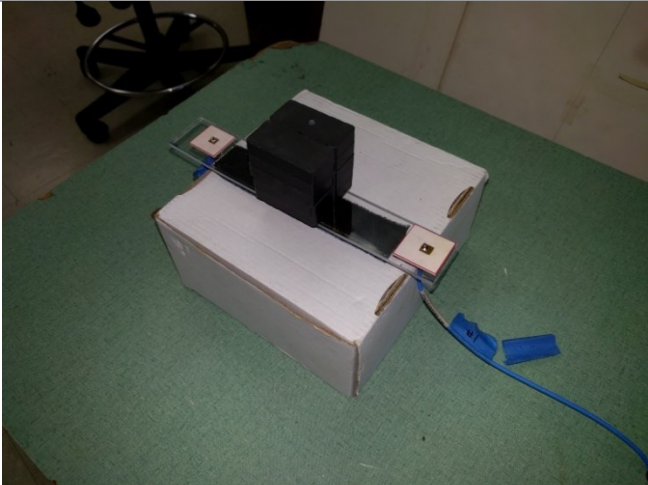
<b>FR4</b>	2.31	
------------	------	--

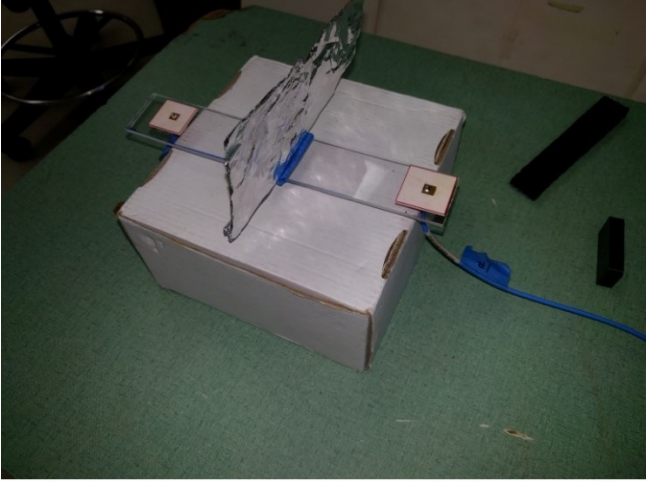
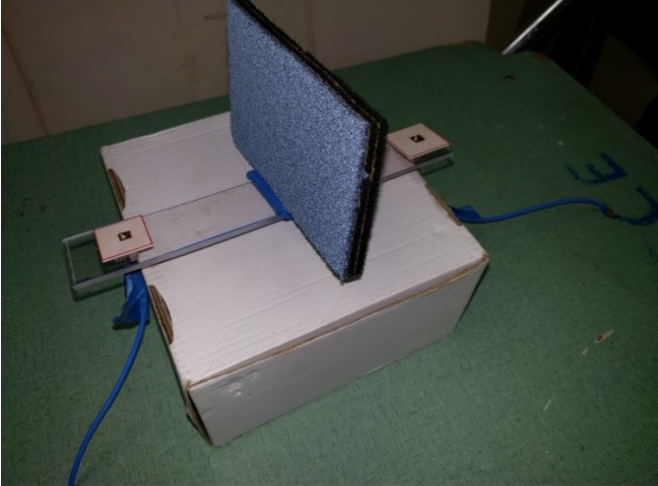
#### 4.1.2 *Physical Testing of Materials*

These materials were also physically tested for their isolation performance. However, given the susceptibility of the test environment to uncontrollable factors and the inconsistencies of the measurements from one test to another, the results were not to be trusted completely. Those results are included here, though the results should be taken as general trends.

In the physical tests, the FR4 performed the best, but as mentioned before, the testing environment was not ideal and therefore the data is subject to scrutiny.

Table 3: Physical testing of barrier materials.

Technique	Increase in Isolation from Control (dB)	Picture
FR4 30 mil Thick, 1oz Cu, 3" Tall	2.8	 <p>FR4 30mil 3in tall 1oz copper</p>
Ferrite Tall Wide Double	2.4	 <p>Ferrite Block 5 Tall Aligned</p>

<b>Foil 3" Tall 4 Sheets Thick</b>	2.0	 <p>Foil Wall 3in tall</p>
<b>Foam Wall 3" Tall</b>	0.4	 <p>Foam Wall 3in</p>

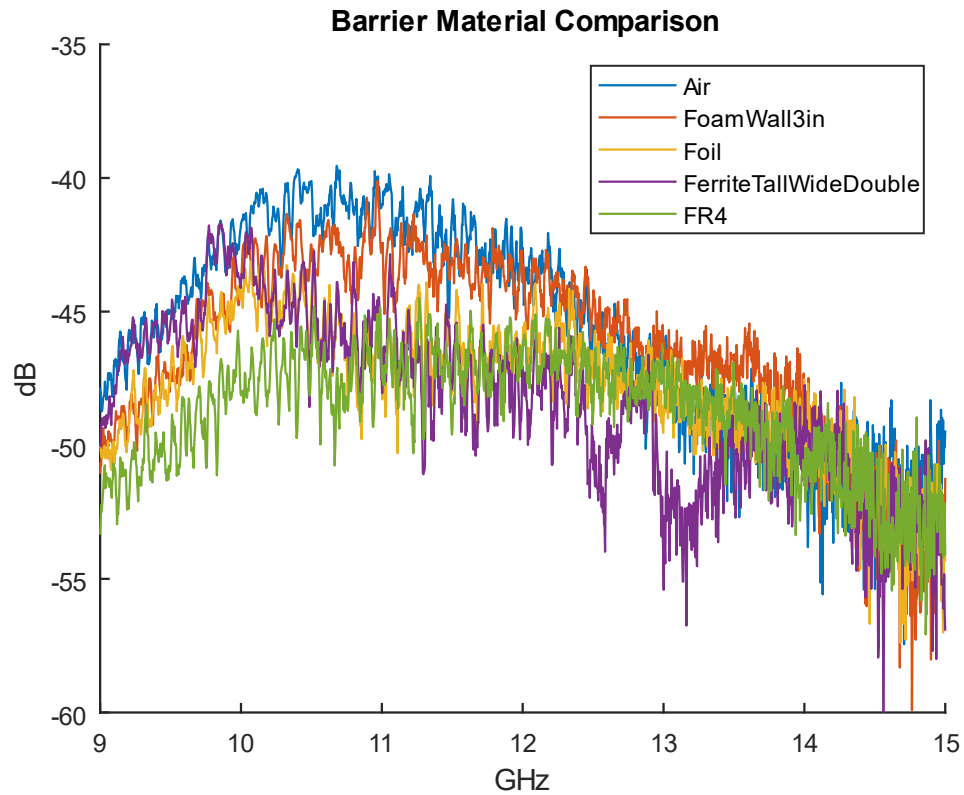


*Figure 4-1: Comparison of coupling by barrier materials. In this test, the FR4 showed the best increase in isolation.*

An inductive wire coil was also tested as a barrier material, but it increased the coupling between the two antennas. The inductor was built by manually winding wire around a hollow cylinder until the desired inductance was achieved. The antennas were then placed within the coil.



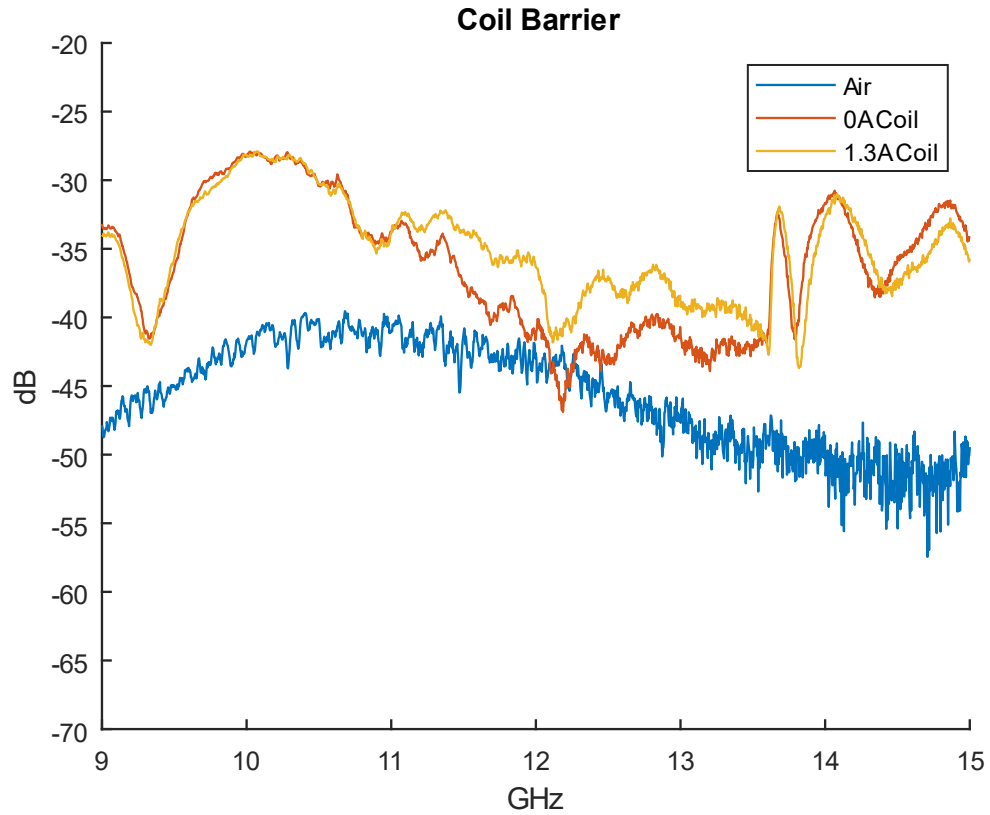


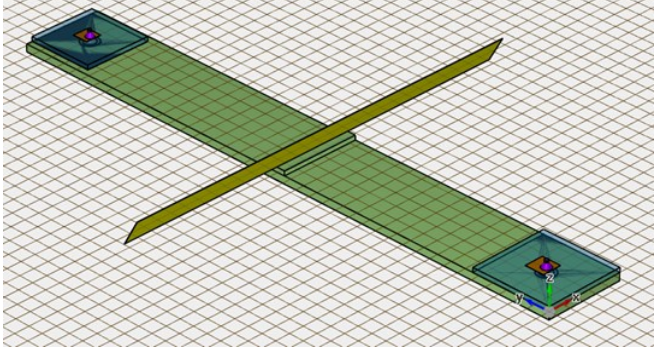
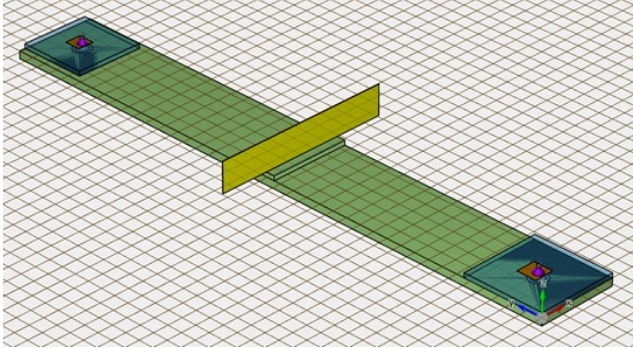
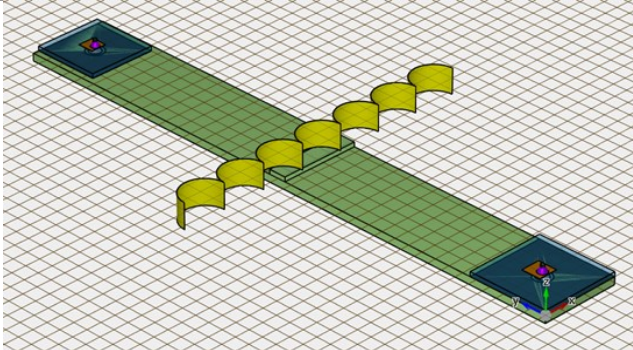
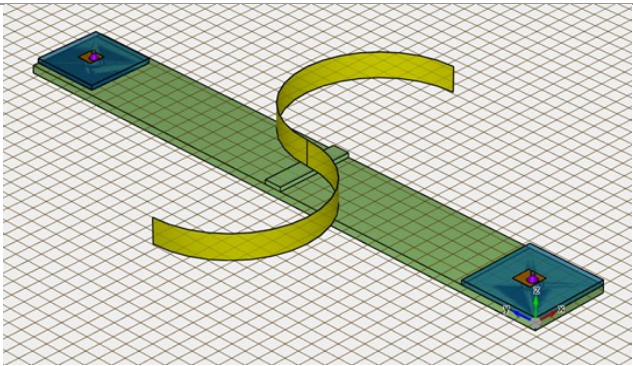
Figure 4-2: Increase in coupling when using an inductive coil.

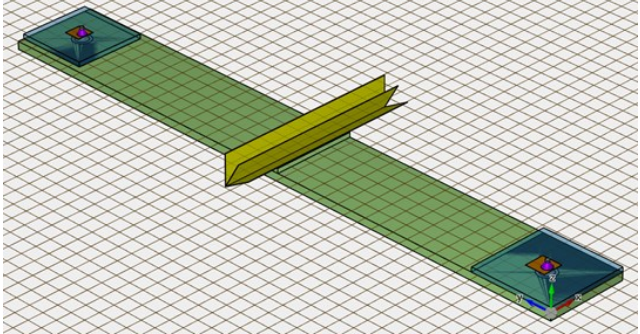
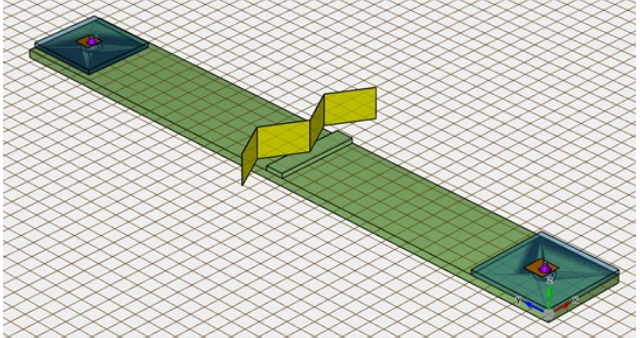
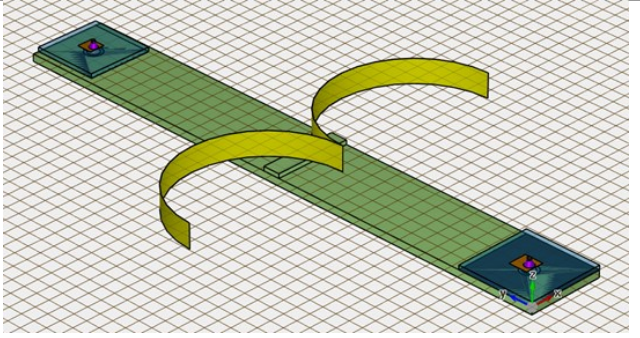
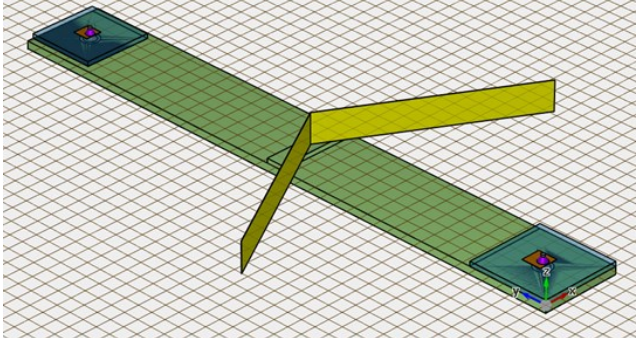
## 4.2 Variation in Barrier Shape

The shape of the barrier is also a factor in how much isolation it provides. Since metal barriers are the easiest to manufacture into different shapes, conductive materials were used as barriers in simulations investigating the effect of shape on isolation. A variety of shapes and configurations were simulated, and the results are included below.

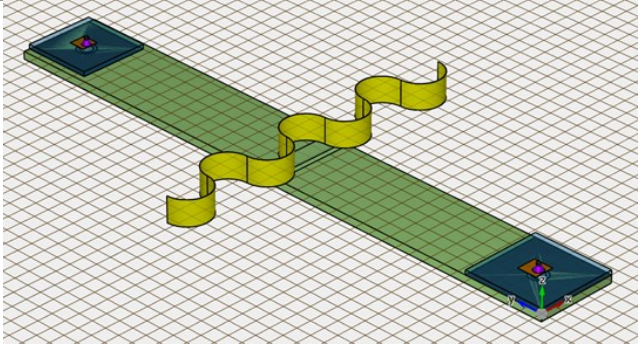
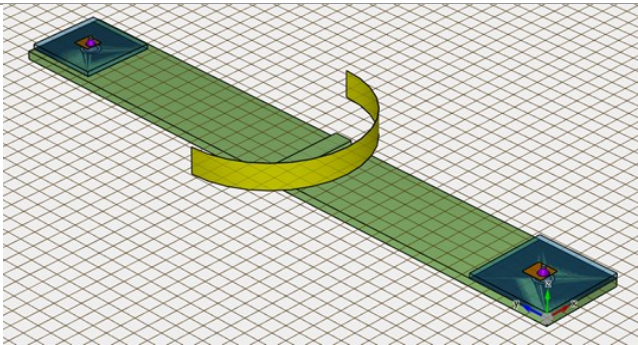


Table 4: Simulation of metal barrier isolation by shape.

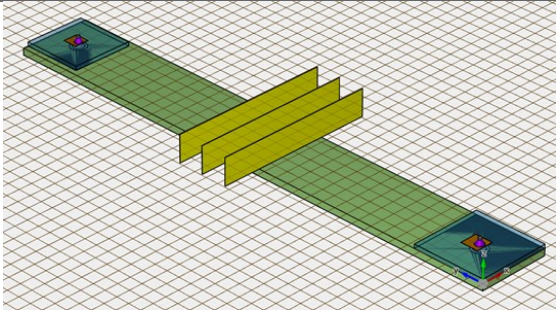
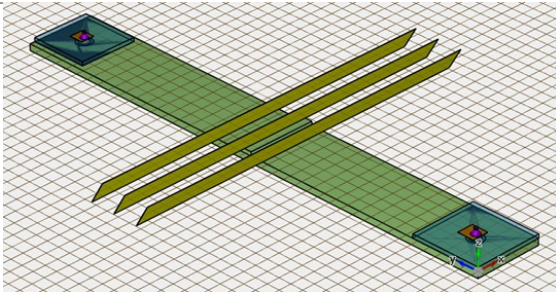
Shape	Increase in Isolation from Control (dB)	Picture
Leaning 30°	7.06	
Straight	5.72	
Smaller Bump	5.39	
S-Shaped	5.28	

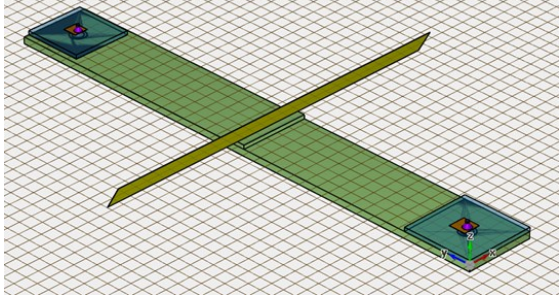
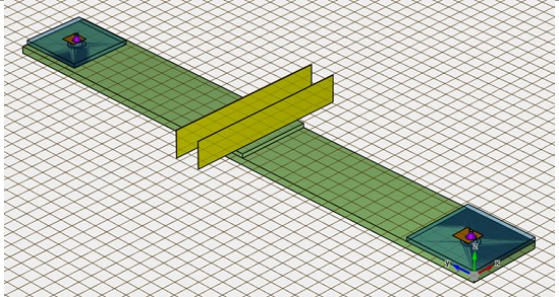
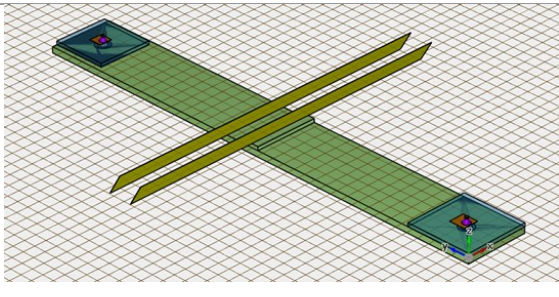
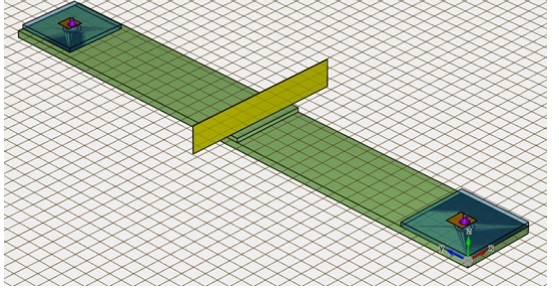
<b>Fan 3 Sheets (90°/60°/30°)</b>	4.94	 A 3D model of a 'Fan 3 Sheets' structure. It consists of a long, narrow green rectangular base with a grid pattern. At each end of the base is a small blue square platform with a red cube on top. A yellow, fan-shaped structure is attached to the center of the base, extending upwards and outwards in a fan-like shape.
<b>W-Shaped</b>	4.91	 A 3D model of a 'W-Shaped' structure. It consists of a long, narrow green rectangular base with a grid pattern. At each end of the base is a small blue square platform with a red cube on top. A yellow, W-shaped structure is attached to the center of the base, extending upwards and outwards in a W-like shape.
<b>Bump</b>	4.91	 A 3D model of a 'Bump' structure. It consists of a long, narrow green rectangular base with a grid pattern. At each end of the base is a small blue square platform with a red cube on top. A yellow, curved structure is attached to the center of the base, extending upwards and outwards in a curved, bump-like shape.
<b>V-Shaped</b>	4.86	 A 3D model of a 'V-Shaped' structure. It consists of a long, narrow green rectangular base with a grid pattern. At each end of the base is a small blue square platform with a red cube on top. A yellow, V-shaped structure is attached to the center of the base, extending upwards and outwards in a V-like shape.



<b>Wave</b>	4.78	
<b>Curved</b>	4.67	

*Table 5: Simulation of metal barrier isolation by configuration.*

<b>Shape</b>	<b>Increase in Isolation from Control (dB)</b>	<b>Picture</b>
<b>Straight (3)</b>	8.20	
<b>Leaning 30° (3)</b>	7.77	

<b>Leaning 30°</b>	7.06	
<b>Straight (2)</b>	7.04	
<b>Leaning 30° (2)</b>	6.59	
<b>Straight</b>	5.72	

In general, the more exotic the shape, the higher the coupling, but the differences were often small. The taller the barrier, the better the isolation, until about 15mm, where there stops being a large difference. A leaning flat conductive sheet provided the best isolation when comparing the single barriers, but regular straight sheets provide the best isolation when using multiple sheets.

### 4.3 Variation in Barrier Placement

After observing that a straight metal barrier provided the most potential to be scaled into a high isolation structure, simulations were conducted to determine an optimum configuration for the test

setup. Copper, steel, and iron barriers were simulated at common thicknesses ranging from 1 mil to 32 mils, and no significant differences were found between these. It was found that the closer the barrier was to the antennas and the greater the number of repeated conductive sheets, the better the isolation between the antennas. Spacing the barriers at wavelength-multiple intervals (half-lambda, quarter-lambda, etc.) did not have a noticeable effect on the isolation. Using an 8 inches long rig for the barriers, the highest number of sheets simulated was 46, producing 21.40 dB isolation.

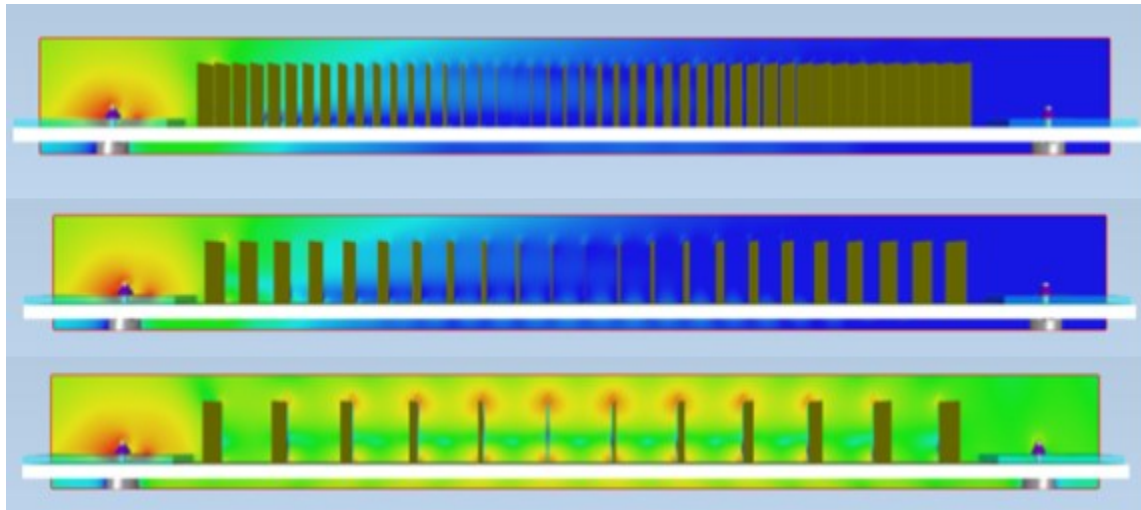


*Figure 4-3: Simulations models of metal grating barrier with variable number of sheets. More of the radiated waves are blocked as the number of sheets increases.*

This metal grating barrier resembles the miniature waveguide barrier discussed in [18], although at more of a macro scale. In this configuration, the repeated metal sheets create parallel-plate waveguides that pull the energy down and away from the receive antenna by diffraction in a manner to that discussed in [1]. The more sheets that could be fit between the two antennas, the more waveguides and the greater the isolation, so long as there is still enough space between the metal sheets that relevant TE modes can be supported.

A final 31-sheet physical barrier was constructed with a 3D printed rig in which the two antennas would be placed, and which had slots to place the conductive barriers. 16 mil copper sheets were cut into 31 pieces  $\frac{1}{4}$ " inch tall and were slotted in as the barrier, spaced 0.15 inches apart. The number of sheets was reduced from the maximum of 46 in simulation to the final quantity of 31 to make construction easier. It was tested using a network analyzer inside of an RF anechoic chamber. The barrier demonstrated an increased isolation of 21dB.



## 5 Isolation by Electromagnetic Band Gap Structures

Electromagnetic band gap structures are periodic elements that exhibit high impedance towards particular frequencies while passing others through as usual, creating a “band-gap” effect. They are modeled after photonic band gap structures typically created in periodic crystals for use in optics. Since large-scale investigations of the structures for RF and microwave applications began in the late 90’s, they have been used to increase performance in many RF and microwave applications, particular regarding patch antenna technology [11]. When incorporated in printed circuit board technology, EBG structures can suppress surface waves in their bandgap, and can therefore increase the isolation between two planar antennas on the same board as demonstrated in [6, 8, 19].

Three common EBG structures will be simulated and compared: the mushroom-like EBG [6], the UC-UBG [7], and the AI-EBG [9]. Each will be designed and simulated to increase isolation between two X-band antennas spaced five wavelengths apart on 60mil RT/Duroid 5880 with 1oz copper. The substrate will be wide enough to accommodate a four by four EBG pattern for each structure. Each will first be designed as a unit cell and characterized using the reflection phase method [11]. In this method, a plane wave is excited normal to the surface of the unit cell. When the phase of the reflected wave is 0 degrees, the unit cell appears as a perfect magnetic conductor and predicts where the center of the bandgap will be. The unit cell will then be simulated in the four by four pattern between the antennas compared to a control simulation where the substrate remains the same size but the EBG structures are removed.

### 5.1 Mushroom-Like EBG

The mushroom-like EBG is one of the earliest proposed EBG structures [11], and it was shown in [6] to increase the isolation between C-band patch antennas. This structure is composed of repeating unit cells that contain a square patch connected to the ground plane by a via in the center.

For this X-band test, the unit cells are tuned to have a reflection phase of 0 degrees at about 10.2 GHz. The square patch is about 0.3 wavelengths across with a gap of 0.1 wavelengths from the patch edge to the unit cell edge.

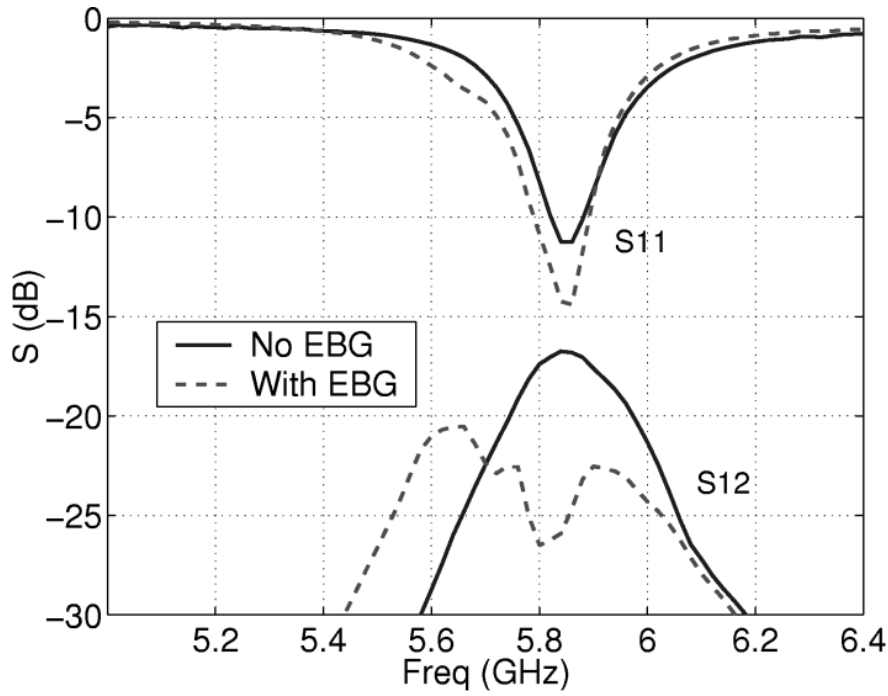


Figure 5-1: Performance of EBG barrier from [10], demonstrating an average decrease in coupling of about 7dB in the band of interest

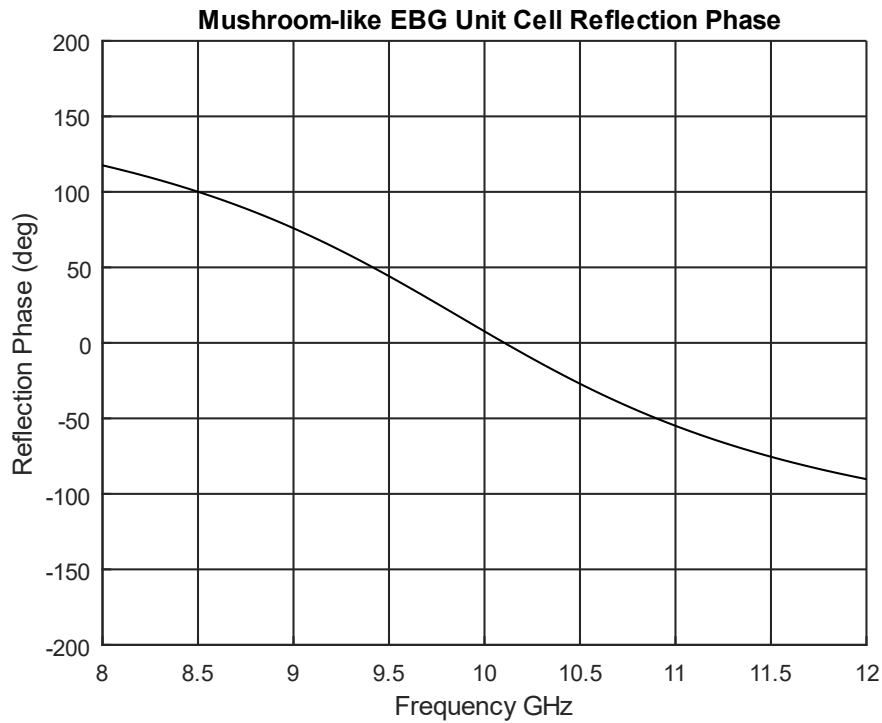


Figure 5-2: Mushroom-like EBG unit cell reflection phase. At a reflection phase of 0, the unit cell acts as a perfect magnetic conductor, indicating where the center frequency of the band gap will be when the unit cell is integrated into a periodic structure.

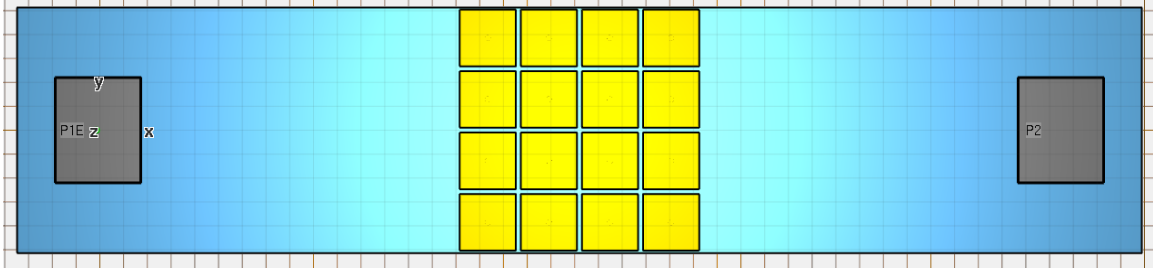


Figure 5-3: Mushroom-like EBG barrier simulation model. Two control antennas are separated by 10 wavelengths and a 4x4 periodic EBG structure.

The mushroom-like EBG unit cell is tuned to approximately 10.2 GHz and placed in a four-by-four lattice between two X-band antennas on the same substrate.

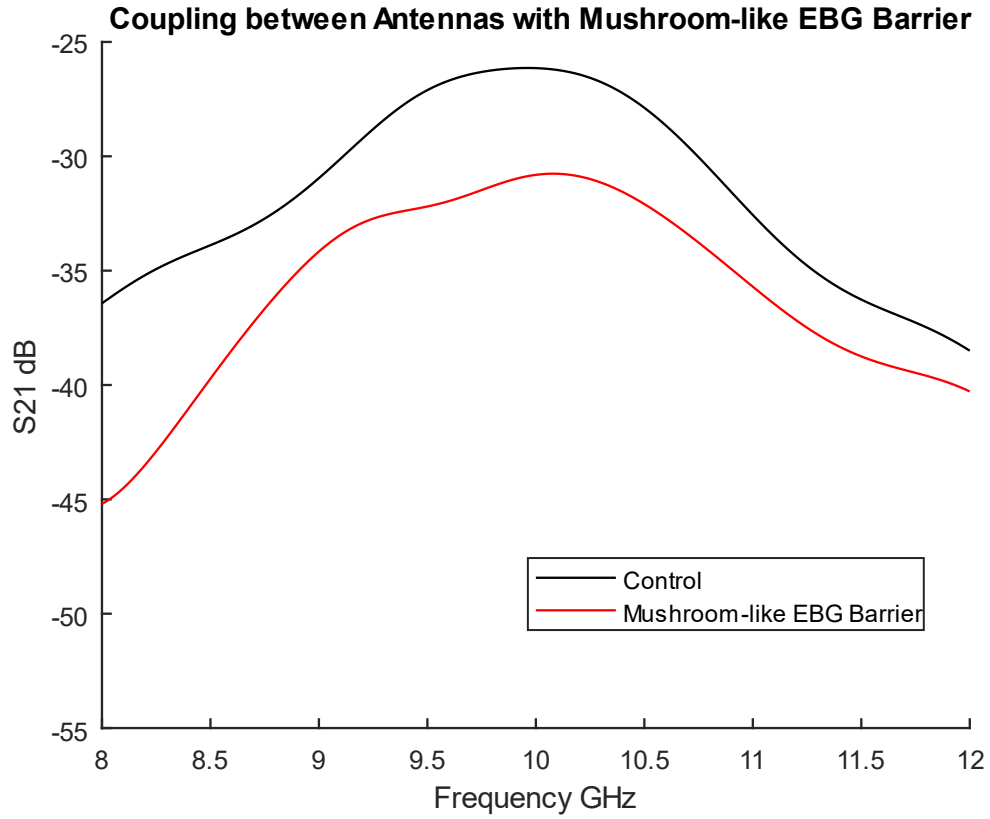


Figure 5-4: Coupling between antennas with mushroom-like EBG barrier. Isolation is increased by an average of 4.4dB over the 10-10.5 GHz band.

The simulated design produced an average of 4.4dB improvement in isolation in the 10-10.5 GHz frequency band. This is less than the 8dB improvement demonstrated in [6], but can be due to their



use of a thicker substrate (75mils), higher dielectric constant (10.2), and implementation on a lower C-Band system.

## 5.2 UC-EBG

The uniplanar compact EBG (UC-EBG) was first proposed in [7]. Unlike the mushroom-like EBG, it does not require vias and is constructed on a single plane. The structure is composed a square metal patch with four connecting branches in a repeating pattern. The narrow connections between unit cells provide inductance, while the gaps between patches provide capacitance, creating the filter-like bandgap.

The unit cell was first designed using a scaled version of the cell presented in [7] and simulated using the reflection phase method [11].

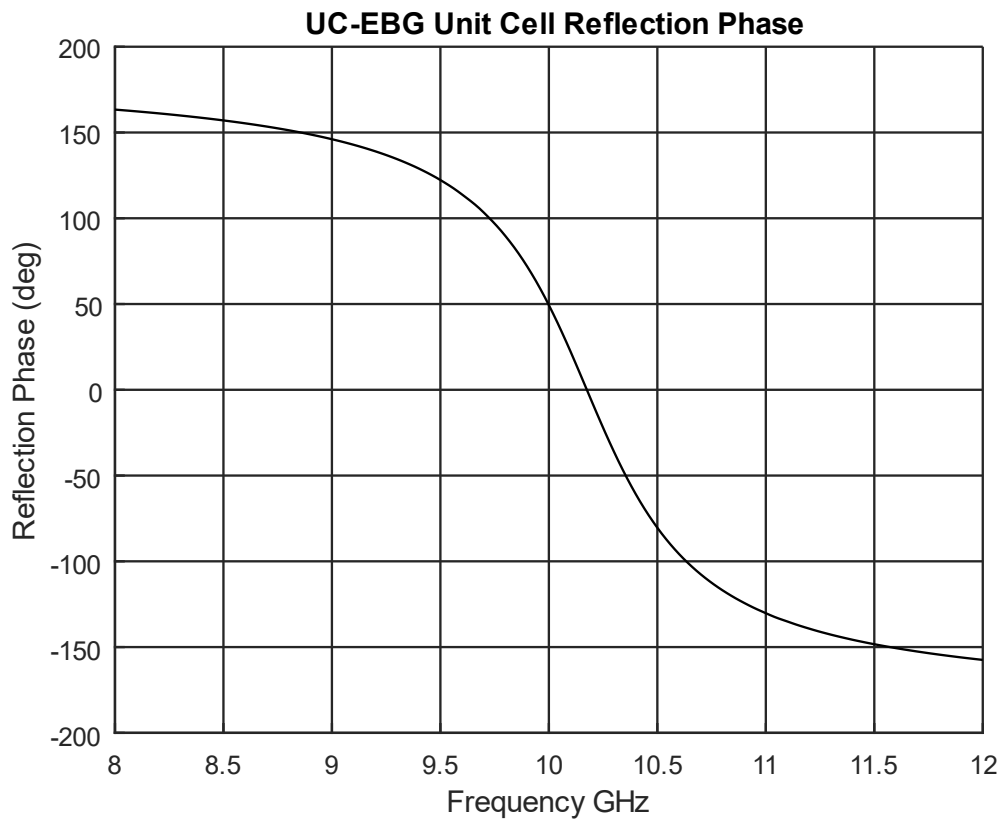


*Figure 5-5: UC-EBG unit cell reflection phase. At a reflection phase of 0, the unit cell acts as a perfect magnetic conductor, indicating where the center frequency of the band gap will be when the unit cell is integrated into a periodic structure.*

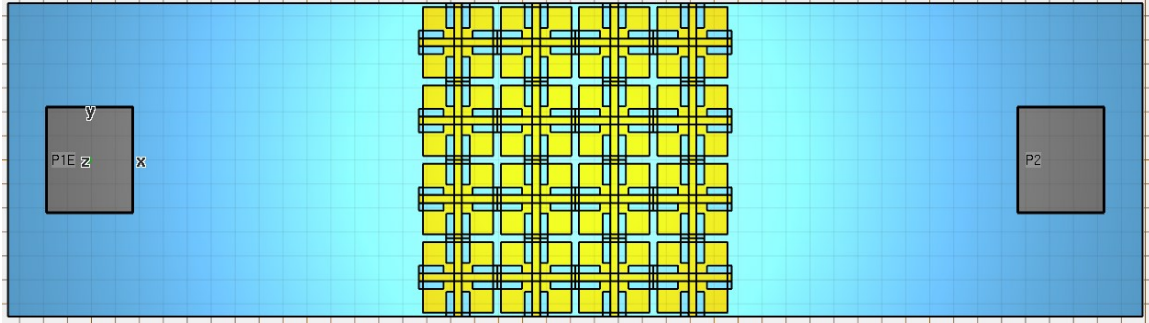


Figure 5-6: UC-EBG simulation model. Two control antennas are separated by 10 wavelengths and a 4x4 periodic EBG structure.

The unit cell is adjusted to a 0 degree reflection phase at 10.2 GHz and placed in a lattice four unit cells deep between two X-band antennas on the same substrate.

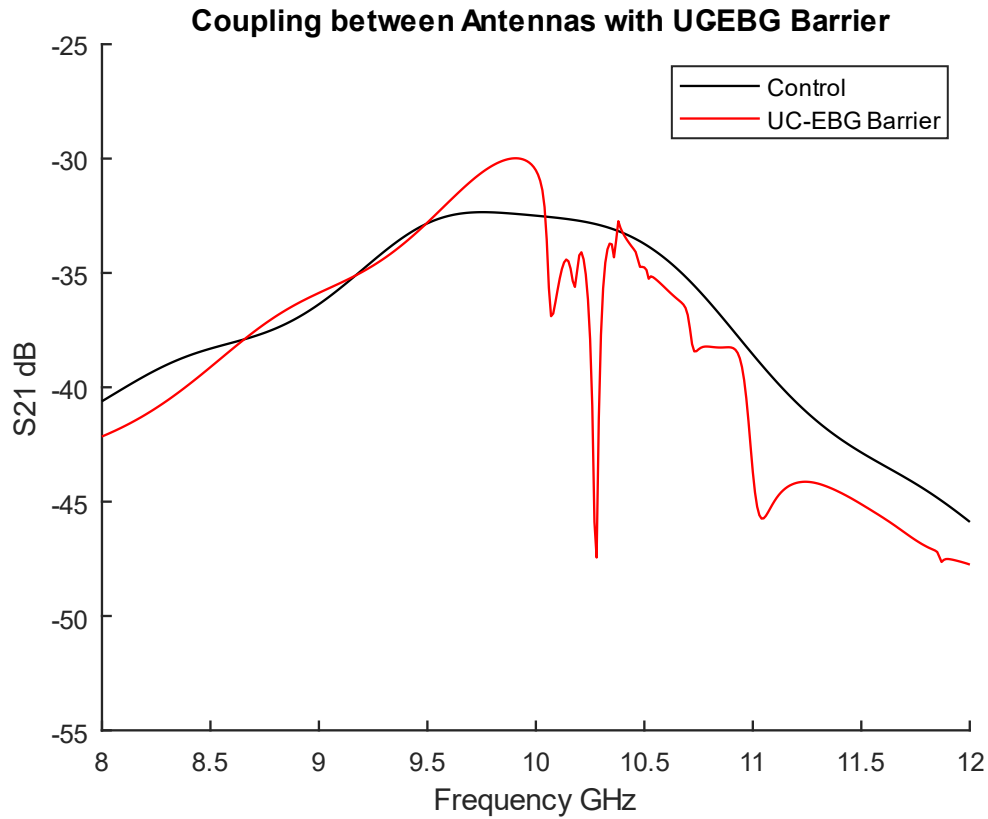


Figure 5-7: Coupling between antennas with UC-EBG barrier. Isolation is increased by an average of 2dB over the 10-10.5 GHz band.

The simulated structure produced a mean increase in isolation of 2dB over the 10-10.5 GHz band. The reject band of the structure is narrower than in the mushroom-like case, but this structure is planar and does not require vias to connect it to the ground plane.

### 5.3 AI-EBG

The alternating impedance EBG (AI-EBG) is described in [9]. Like the UC-EBG, it is a uniplanar pattern formed by square patches connected by small branches. In this pattern, all of the patches and branches are square, the patches being approximately 0.5 wavelengths across and the branches approximately 0.1 wavelengths across. The different impedances produced by the two different sizes create the bandgap.

The unit cell was first designed and simulated using the reflection phase method [11].

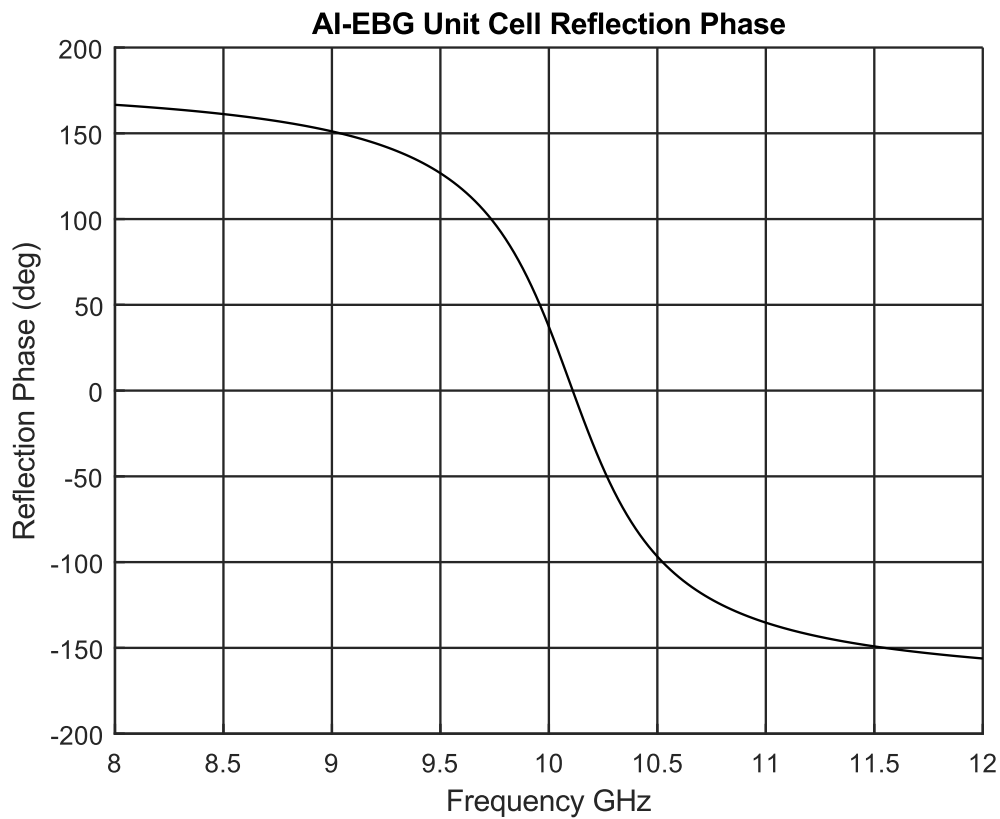


*Figure 5-8: AI-EBG unit cell reflection phase. At a reflection phase of 0, the unit cell acts as a perfect magnetic conductor, indicating where the center frequency of the band gap will be when the unit cell is integrated into a periodic structure.*

The unit cell is tuned to approximately 10.2 GHz and placed in a lattice four unit cells deep between two X-band antennas on the same substrate.

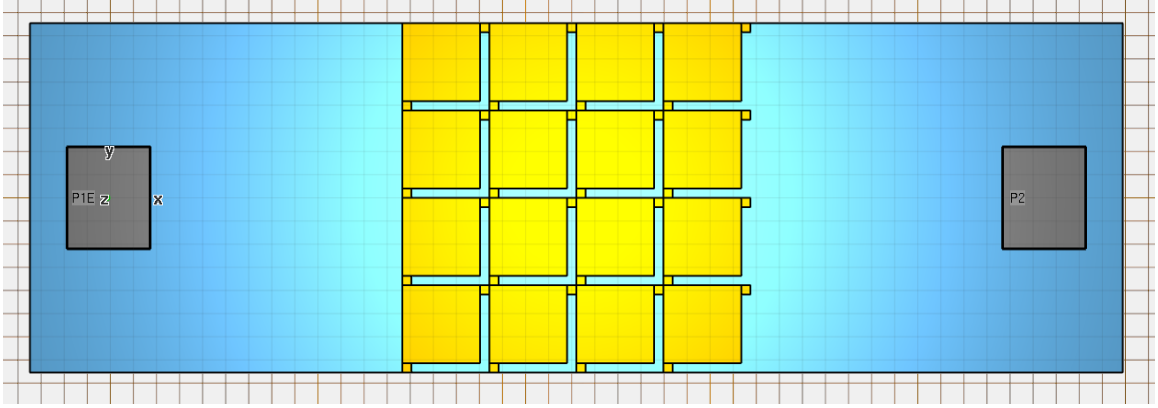


Figure 5-9: AI-EBG simulation model. Two control antennas are separated by 10 wavelengths and a 4x4 periodic EBG structure.

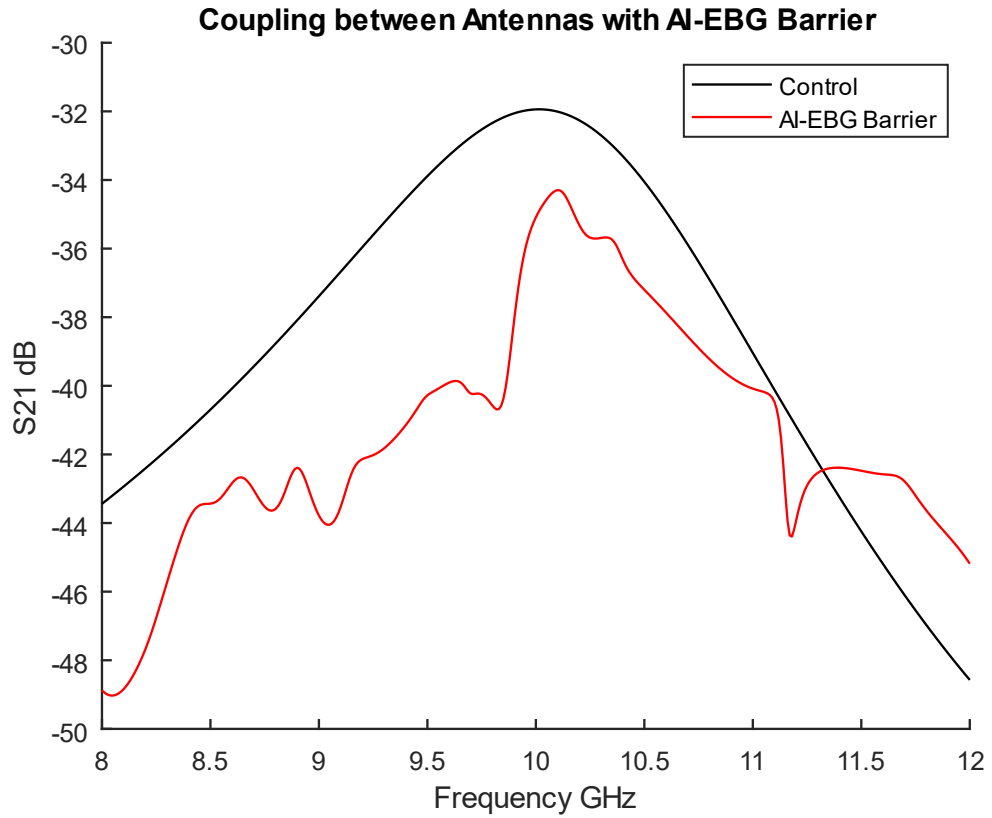


Figure 5-10: Coupling between antennas with AI-EBG Barrier. Isolation is increased by an average of 2.9dB over the 10-10.5 GHz band.

The simulated design produced a 2.0dB improvement in isolation at the center frequency of 10.25 GHz and a mean improvement of 2.9dB over the 10-10.5 GHz band.



## 6 Comparison of the Investigated Techniques

The several techniques presented have been analyzed for antennas in the X-band. They are presented below in order of their effectiveness in increasing isolation. Note that there is a mix of actual hardware tests and simulations, and the spacing between the antennas varies from one wavelength to ten wavelengths. Of course, simply increasing the distance between the antennas and disconnecting them from each other will provide the greatest improvement in isolation and should be done whenever possible. When not possible, the discussed solutions should be among those considered.

*Table 6: Comparison of isolation techniques*

Technique	Increase in Isolation (dB)
<b>Defected Ground Plane Filter</b>	25.8
<b>Metal Grating Barrier</b>	21
<b>Defected Microstrip Filter</b>	10
<b>Mushroom-Like EBG Barrier</b>	4.4
<b>AI-EBG Barrier</b>	2
<b>UC-EBG Barrier</b>	2
<b>Via Walls</b>	-0.7

Of the above techniques, the defected ground plane filter demonstrated the greatest increase in isolation, while the via walls decreased the isolation. Unfortunately, the DGS as well as the DMS filters cannot be used if the desired Rx signal lies in the same band as the Tx signal. In that case, they will also reject the desired signal.

For systems whose Rx and Tx bands are the same or overlapping, the metal grating barrier displays the best isolation. However, because this barrier is not planar, it obstructs the radiation pattern of the antennas and warps them away from the barriers. This may not be desirable for antennas intended to be omnidirectional or for antennas meant to be steered.

As the via walls have been shown in simulation to decrease isolation, the EBG barriers show the most promise for increasing isolation while not affecting the antennas. This comes at the cost of being much less effective methods than the other techniques, but they may be the only option in some high-sensitivity applications where every bit of extra isolation matters.



## 7 Conclusions

This thesis has explored uncommon hardware design techniques for isolating closely spaced planar X-band antennas. Each of the techniques investigated is completely passive and requires no expensive components, processing capability, or power. Because of this, they can be readily implemented to improve existing systems without major detriment to other subsystems, so long as size and physical system geometry permits their use. The levels of isolation demonstrated are very high for planar structures without closed waveguides.

With the exception of the metal grating barrier, the techniques are not new to decoupling in general, in that there is existing literature on their use for at least one application. None of the reviewed literature applied the solutions to X-band systems, and so this work has shown that these solutions still improve isolation when scaled to a different frequency. However, every real-world system has a different configuration and challenges unique to itself. Not all of the presented solutions will be implementable in every system, and it is therefore the responsibility of the engineer to determine which solution or solutions should be used for their system.

### 7.1 Further Research

The solutions presented are in no way the entirety of the problem's solution space. EBG structures alone are still being investigated and improved upon today, decades after their first proposal. With further research and tuning, the performance of the X-band EBG barriers can likely be increased to match the 10dB+ isolation of their lower frequency counterparts presented in [6-7, 9], and that same research can be applied to the EBG-like defected ground plane and defected microstrip filters. Their development and performance suggest that metamaterial-like solutions are the future of decoupling solutions, such as is used in [18], but the field of metamaterials will likely need to mature more before their products can be used to solve coupling problems between X-band antennas at an economical scale.



## References

- [1] L. S. Riggs and D. A. Vechinski, "A Radio Frequency (RF) Barrier Effectiveness Assessment Study," *IEEE 1988 International Symposium on Electromagnetic Compatibility*, pp. 368-372, 1988.
- [2] S. Tokumaru, S. Sakuda and K. Nagai, "A method of decoupling in two folded unipoles," in *1976 Antennas and Propagation Society International Symposium*, Amherst, MA, USA, 1976.
- [3] J. Juntunen and J. Rahola, "Dual-band lumped element decoupling network design for two-antenna systems," in *2017 11th European Conference on Antennas and Propagation (EUCAP)*, Paris, 2017.
- [4] J. Hoffman, "Decoupling flush-mounted slot antennas in a common ground plane," in *1964 Antennas and Propagation Society International Symposium*, Long Island, NY, USA, 1964.
- [5] M. A. Tilston, S. E. Tilston and W. V. Tilston, "The coupling and decoupling of closely spaced antennas," in *33rd IEEE Vehicular Technology Conference*, Toronto, ON, Canada, 1983.
- [6] F. Yang and Y. Rahmat-Samii, "Microstrip Antennas Integrated With Electromagnetic Band-Gap (EBG) Structures: A Low Mutual Coupling Design for Array Applications," *IEEE Transactions on Antennas and Propagation*, vol. 51, no. 10, pp. 2936-2946, 2003.
- [7] F.-R. Yang, K.-P. Ma and Y. Qian, "A Uniplanar Compact Photonic-Bandgap (UC-PBG) Structure and Its Applications for Microwave Circuits," *IEEE Transactions on Microwave Theory and Techniques*, vol. 47, no. 8, pp. 1509-1514, 1999.
- [8] X. Yang, Y. Liu, Y. Xu and S. Gong, "Fractal UC-EBG structure and cross slot for mutual coupling suppression applications," *2017 International Applied Computational Electromagnetics Society Symposium (ACES)*, pp. 1-2, 2017.

- [9] J. Choi, V. Govind and M. Swaminathan, "A novel electromagnetic bandgap (EBG) structure for mixed-signal system applications," in *2004 IEEE Radio and Wireless Conference (IEEE Cat. No.04TH8746)*, Atlanta, GA, 2004.
- [10] A. Aminian, F. Yang and Y. Rahmat-Samii, "In-phase reflection and EM wave suppression characteristics of electromagnetic band gap ground planes," *IEEE Antennas and Propagation Society International Symposium. Digest. Held in conjunction with: USNC/CNC/URSI North American Radio Sci. Meeting (Cat. No.03CH37450)*, vol. 4, pp. 430-433, 2003.
- [11] M. S. Alam, N. Misran, B. Yatim and M. T. Islam, "Development of Electromagnetic Band Gap Structures in the Perspective of Microstrip Antenna Design," *International Journal of Antennas and Propagation*, 2013.
- [12] M. K. Mandal and S. Sanyal, "A novel defected ground structure for planar circuits," *IEEE Microwave and Wireless Components Letters*, vol. 16, no. 2, pp. 93-95, Feb. 2006.
- [13] D. Ahn, J. S. Park, C. S. Kim, J. Kim, Y. Qian and T. Itoh, "A design of the low-pass filter using the novel microstrip defected ground structure," *IEEE Transactions on Microwave Theory and Techniques*, vol. 49, no. 1, pp. 86-93, January 2001.
- [14] C.-S. Kim, J.-S. Lim, S. Nam, K.-Y. Kang and D. Ahn, "Equivalent circuit modelling of spiral defected ground structure for microstrip line," *Electronics Letters*, vol. 38, no. 19, pp. 1109-1110, 12 Sept. 2002.
- [15] J. W. Kunzler, J. M. Bartschi and K. F. Warnick, "Compact structure with high TX-RX isolation for frequency domain duplexing on printed circuit boards," *Journal of Electromagnetic Waves and Applications*, vol. 34, no. 3, pp. 390-395, 28 Jan 2020.
- [16] D.-J. Woo, T.-K. Lee, J.-W. Lee, Pyo Cheol-Sig and W.-K. Choi, "Novel U-slot and V-slot DGSs for bandstop filter with improved Q factor," *IEEE Transactions on Microwave Theory and Techniques*, vol. 54, no. 6, pp. 2840-2847, June 2006.
- [17] D. La, Y. Lu and S. Sun, "Novel bandstop filter using dual-U shape defected microstrip structure," *2010 International Symposium on Signals, Systems and Electronics*, pp. 1-3, 2010.

- [18] A. U. Zaman, M. S. Ellis and P.-S. Kildal, "Metamaterial based packaging method for improved isolation of circuit elements in microwave modules," *2012 7th European Microwave Integrated Circuit Conference, Amsterdam*, pp. 834-837, 2012.
- [19] Y. Su, L. Xing, Z. Z. Cheng, J. Ding and C. J. Guo, "Mutual coupling reduction in microstrip antennas by using dual layer uniplanar compact EBG (UC-EBG) structure," *2010 International Conference on Microwave and Millimeter Wave Technology*, pp. 180-183, 2010.